DE GRUYTER

Biologia **72**/4: 398—406, 2017
Section Botany
DOI: 10.1515/biolog-2017-0041

Type II metacaspase protein localization and gene transcription during programmed cell semi-death of sieve elements in developing caryopsis of *Tritium aestivum**

Zhihui Zhang[1], Yani Lv[1], Zhuqing Zhou[1]**, Fangzhu Mei[2] & Likai Wang[1]

[1]*Laboratory of Cell Biology, College of Life Science and Technology, Huazhong Agricultural University, Wuhan, Hubei 430070, China; e-mail: zhouzhuqing@mail.hzau.edu.cn*
[2]*College of Plant Sciences & Technology, Huazhong Agricultural University, Wuhan, Hubei 430070, China*

Abstract: Metacaspases are cysteine-dependent proteases essential in plant PCD. This study focused on PCD features, the metacaspase II protein (TaeMCAII) and its gene expression and dynamic distribution during the developmental process of wheat sieve elements (SEs). Our results showed that the SEs experienced enucleation, inclusion loss, cell wall thickening and decreased cytosol density during their development. The RT-qPCR and *in situ* hybridization showed that the transcriptional levels of TaeMCAII in the development of SEs increased to high levels 3 days after flowering (DAF), then decreased, but then sharply increased at 7 DAF. Immunohistochemical observations revealed dynamic changes of TaeMCAII at the protein level. TaeMCAII was primarily detected at 3 DAF, 4 DAF and 7 DAF, which indicated that TaeMCAII played an important role during these stages. Immunoelectron microscopy showed that TaeMCAII was first localized in the nucleus, then in the cell cytoplasm, and finally on the cell membranes and cell walls of late-stage SEs. Our study found that TaeMCAII was key in the PCD-like process of the development of SEs.

Key words: *Triticum aestivum* L.; sieve elements; programmed cell death; immunoelectron microscopy; TaeMCA II.

Introduction

Phloem consists of SEs, companion cells and parenchymatic cells in monocotyledon. The main role of phloem is to transport photoassimilate to necessary parts of the plant, such as the buds, root tips, fruits and seeds. Our previous study found that SEs exhibited typical programmed cell death (PCD) characteristics during its development, such as the partial inclusion degradation (Zhou et al. 2004), DNA laddering, cell vacuolization, cell wall thickening and nuclear chromatin condensation (Wang et al. 2008). After nuclear degradation, the vacuole structure was intact, and the cytoplasm that was embedded into vacuoles though the tonoplast retraction was degraded by a hydrolase, such as aspartic proteinase. The tonoplast and plasma membranes fused together to preserve some of the organelles and cytoplasm in the late stages of the development of the SEs (Yang 2013). Recently, an endonuclease, named BEN1-LIKE, was discovered to play a pivotal role in the degradation of the nucleus in the developmental process of wheat SEs (Cai et al. 2015). Prior studies found that the SEs remained active after experiencing the PCD-like process, and therefore the occurrence of this special PCD process experiencing the PCD-like process was named "programmed cell semi-death, an arrested cell death in which a small amount of organelles is retained" (Van Bel 2003).

PCD, which exhibits an active and orderly process of cell death, is a metabolic process in the normal physiological response during the growth and development of an organism (Pennell & Lamb 1997). Caspases-cysteine-dependent aspartate-directed proteases were reported to play essential roles in animal PCD (Earnshaw et al. 1999), but their orthologous proteins in plants have not been found. The existences of distant caspase relatives, named caspase-like proteases, were found in plant cells undergoing PCD (Sanmartin et al. 2005). Metacaspases, as caspase-like enzymes, were discovered in protozoa, fungi and plants. Based on their sequences and structural features, metacaspases were classified as type I, type II (Uren et al. 2000), and more recently, type III (Choi & Berges 2013). Similar to caspase, metacaspases have a characteristic amino acid dyad-cysteine/histidine in the active center and participate in the process of catalysis (Sanmartin et al. 2005), but metacaspases and caspases differ in their substrate specificity (Piszczek & Gutman 2007). Meta-

* Electronic supplementary material. The online version of this article (DOI: 10.1515/biolog-2017-0041) contains supplementary material, which is available to authorized users.
** Corresponding author

caspases are multifunctional proteins that take part in the regulation and executions of PCD, cell cycle control, aging and oxidative stress (Tsiatsiani et al. 2011). For example, a type II metacaspase, mcII-Pa, was reported to be involved in the development of PCD during the early stages of embryogenesis in the gymnosperm plant Norway spruce (*Picea abies*) (Bozhkov et al. 2005; Suarez et al. 2004). Type-II metacaspase cDNA sequences from wheat were cloned, and the experiments showed that the protease (TaeMCAII) was involved in the programmed cell death process under the abiotic stress conditions (Piszczek et al. 2011).

Cells experiencing the PCD process in plants often exhibit increased Ca^{2+} concentrations, nuclear DNA fragmentation, protein phosphorylation, nuclear heterochromatin and ROS (Jones & Dangl 1996). Ca^{2+} not only activates sendonuclease to promote DNA fragmentation, but also breaks the integrity of chromosomes by activating phosphatases and phospholipase. As such, the continuous rise of Ca^{2+} concentrations in the nucleus was considered to be the leading reason for PCD in cells (Sun 1998). The change of the Ca^{2+} concentrations in cells promotes vacuole rupture, which leads to chromatin condensation, and eventually to PCD (Jones 2001). To date, most metacaspases studied required Ca^{2+} for *in vitro* activity (Bozhkov et al. 2005; McLuskey et al. 2012; Piszczek et al. 2012; Watanabe & Lam 2011b; Wong et al. 2012; Zhang & Lam 2011). Until now, the subcellular localization of metacaspase was found only for Arabidopsis metacaspase AtMCP1b and in chloroplasts (Castillo-Olamendi et al. 2007). Although several molecular components of PCD pathways were recently identified in non-metazoan organisms, the role of metacaspase in these pathways is not understood (Tsiatsiani et al. 2011). Our previous work found that the expression levels of the gene encoding TaeMCAII increased in the PCD process of wheat endosperm under waterlogging stress. This demonstrated that TaeMCAII might contribute to the occurrence of PCD. Our objective in this study was to determine whether TaeMCAII also plays a role during in the development of SEs that exhibits typical PCD characteristics in wheat caryopsis (Guo 2013). We adapted a RT-qPCR and an in-situ hybridization approach to study the dynamic changes of gene encoding TaeMCAII at the transcriptional level in the development of SEs, and then localized the protein at the cellular and subcellular levels.

Material and methods

Materials and sampling

The sampling was followed Yang's method (Yang et al. 2015). Wheat (*Triticum aestivum* L.) seeds of cv. Huamai 8 were planted in a greenhouse (12 h light/12 h dark, 20 ℃) of Huazhong Agricultural University, Hubei Province, China. At the time of flowering, the flowering spikelets were tagged with a pen mark on the arista and the ears were tagged with labels. Spikelet samples were collected daily from 0 to7 days after flowering (DAF) for experiment.

Microstructural and ultrastructural observations

The microstructure of the vascular tissue in the caryopses was determined according to Wang's method (Wang et al. 2008) with modifications. Sections were cut on an LKB 2088 Ultracut ultramicrotome (Bromma, Sweden). The sections were then stained with a 0.5% (w/v) toluidine blue solution for 1 min at 25 ℃ and rinsed with ddH_2O. The sections were viewed with a light microscope (Nikon Eclipse 80i, Japan). Statistics were determined for the number changes of the SEs from 0 to 7 days. The ultrastructure of the vascular tissue in the caryopses was determined according to Xu's method (Xu et al. 2013). Sections (80–90 nm thick) were cut on an ultramicrotome and viewed with a transmission electron microscopy (TEM) (H-7650, Hitachi, Japan) at 80 kV.

Terminal deoxynucleotidyl transferase-mediated dUTP nick end labeling (TUNEL)

The TUNEL assays were a valuable indicator of hydrolyzed DNA *in situ* and were conducted according to the manufacturer's instructions (PromegaG3250, Madison, WI, USA) with modifications. Paraffin sections were viewed using a fluorescence microscope (Nikon Eclipse 80i, Japan) under blue-light excitation and were photographed. Green fluorescence (TUNEL-labelling) indicated TUNEL-positive nuclei. Then, the same sections with the propidium iodide staining were viewed using a fluorescence microscope under red-light excitation and photographed, and images of cellular structures were observed using a light microscope (Nikon Eclipse 80i, Japan).

Molecular analysis

Total RNA was extracted using a trizol reagent (Invitrogen). Two micrograms of RNA were reverse-transcribed using the transScript One-Step gDNA Removal and cDNA Synthesis SuperMix kit (Transgen). Quantitative real-time PCR experiments were executed on a StepOne™ Real-time PCR System (Applied Biosystems, USA) using a Top Green qPCR SuperMix (transgen) with specially designed primers. The relative expression level of the gene was quantified with the comparative threshold cycle method, using wheat β-actin as the internal reference. Three technical replication reactions were set up for each sample. Primers for specific genes were as follows: for β-actin (accession no. AB181991): forward 5'-cagcaatgtatgtcgcaatc-3'and reverse 5'-tagcatgaggaagcgtgtat-3'; For TaeMCAII (accession no. ACY82389) forward 5'-atgaaggtgcatcaggtgag-3'and reverse 5'-cccatatcttgtatcgccg-3'.

In situ hybridization

The *in situ* hybridization was adapted from Cai's method (Cai et al. 2015). Oligonucleotides were labeled according to the DIG Oligonucleotide Tailing Kit (Roche, Germany). Immunological detections were performed by the alkaline phosphatase-conjugated anti-digoxigenin antibody and visualized with NBT/BCIP (Roche, Germany). A positive reaction was monitored by observing the development of a blue stain under the light microscope (Nikon Eclipse 80i, Japan).

Immunohistochemistry of TaeMCAII

Immunohistochemistry tests were conducted using Hao's method (Hao et al. 2008). The paraffin embedded samples were cut on a paraffin slicing machine (Leica RM 2235, Germany) at 8 μm. The sections were deparaffinized in xylene and rehydrated. For the immunolabeling, the sections were first rinsed with phosphate-buffered saline (PBS, pH 7.2) for 5 min at room temperature and then incubated in 3%

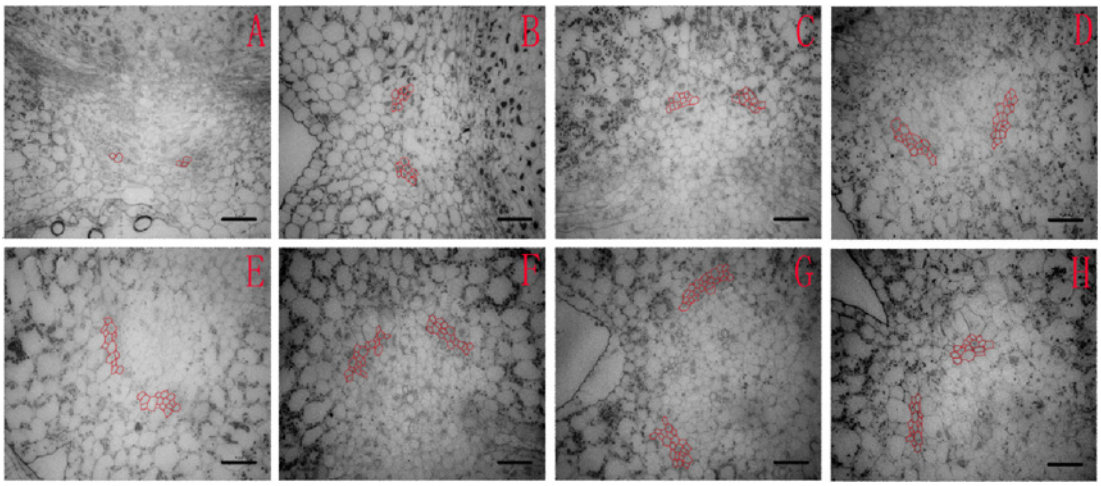

Fig. 1a. Microstructure of the SEs in wheat caryopsis. A–H represent the cross section of wheat caryopsis at 0 DAF–7 DAF respectively. The red curve shows the SEs clusters. Bar: 5 μm.

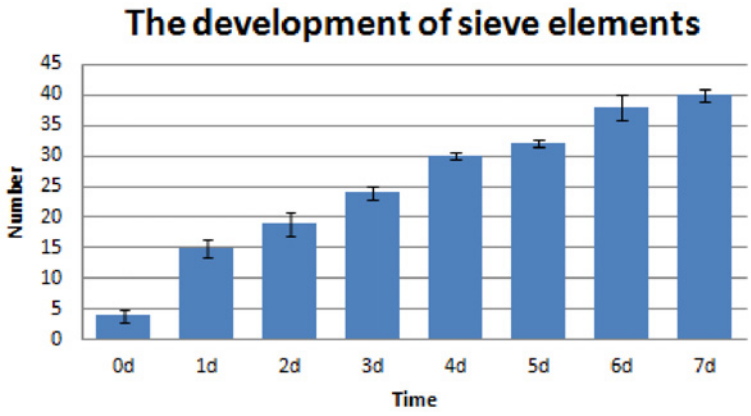

Fig. 1b. The quantitative of the SEs from 0 DAF to 7 DAF.

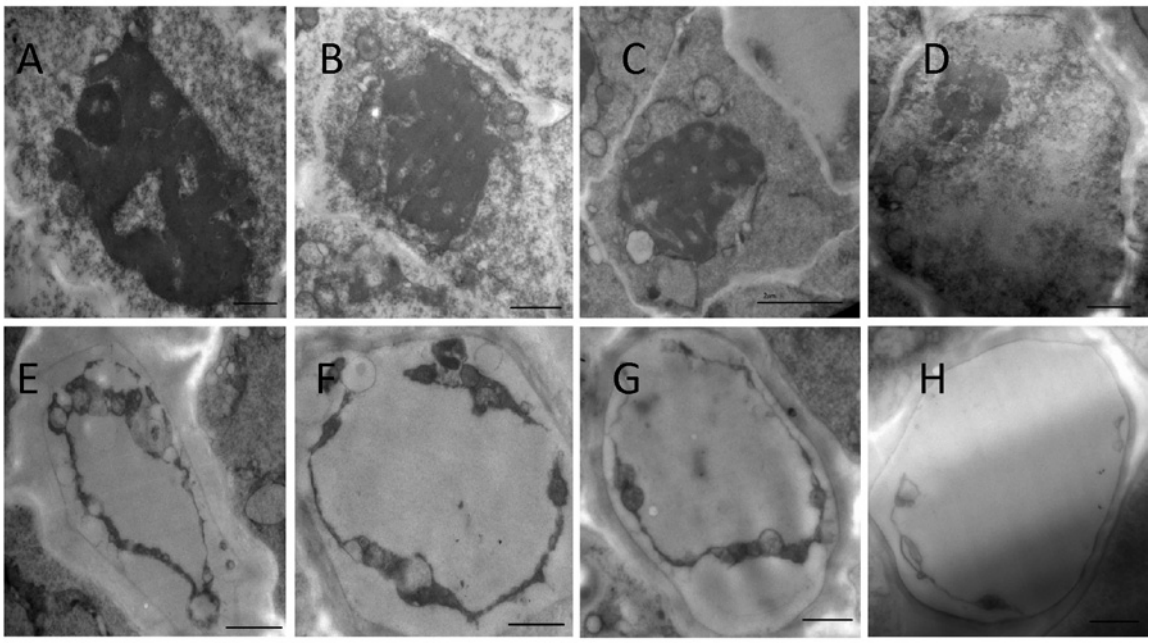

Fig. 2. Ultrastructural observation the SEs in wheat caryopses. A and B represent the SEs at 0 DAF and 1 DAF respectively, the nucleus has a normal appearance. C: 2 DAF SEs, the nuclear structure is modified and chromatin condensation. D: 3 DAF SEs, the nucleus degradation further continued. E: 4 DAF SEs, the cell lost its entire nucleus, the inclusions wrapped in vesicles and vacuoles. F: 5 DAF and G: 6 DAF SEs, the residual portion of the mitochondria and vesicles which close to the plasma membrane, and fusion. H: 7 DAF, the SEs mature and a few organelles are reserved. Bar: 1 μm (A, B, D, E, F, G, H). Bar: 2 μm (C).

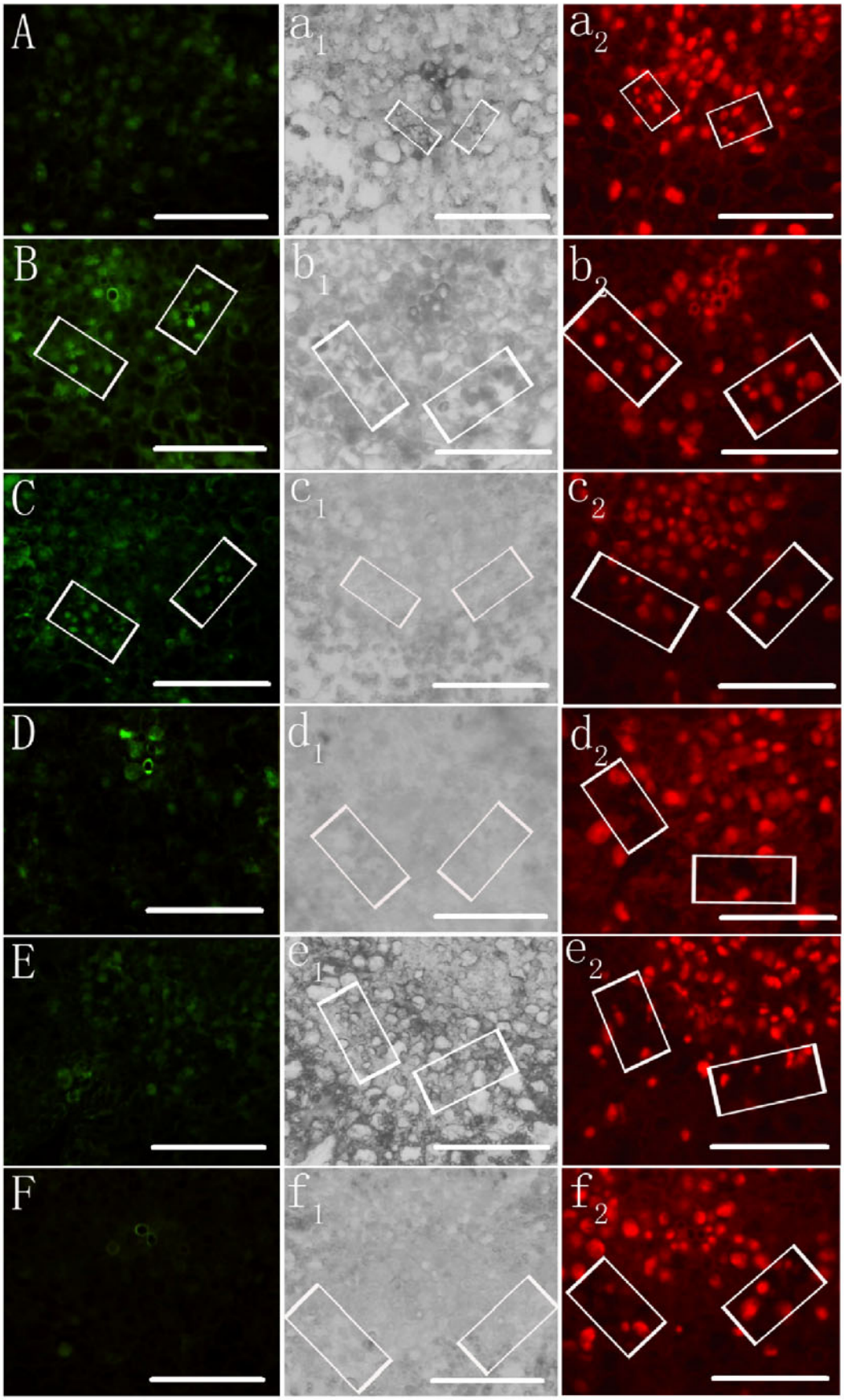

Fig. 3. Terminal deoxynucleotidyl transferase-mediated dUTP nick-end labeling (TUNEL) assays performed on SEs revealed DNA fragmentation during the development process. A–F represent cross section 2–7 DAF SEs respectively (the green fluorescence indicates DNA fragmentation). a_1–f_1 represent cross section 2–7 DAF in the light microscope, respectively. a_2–f_2 represent PI stained cross section 2–7 DAF in the PI staining (the red fluorescence signifies the all nucleus), the white boxes show the SEs. Bar: 10 μm.

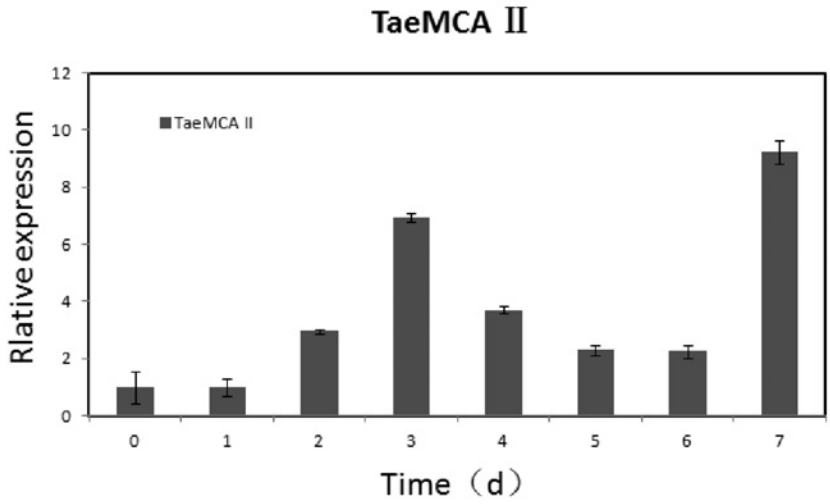

Fig. 4. The expression levels of TaeMCAII mRNA in SEs of wheat caryopses. 0–7 represent the SEs at 0 DAF to 7 DAF, respectively. Transcripts from the control (0 DAF) were taken as 100%. Data are the mean ± SD, n = 3.

H_2O_2 for 10 min. After being blocked in a bovine serum albumin (BSA, Sigma-Aldrich, USA) solution at room temperature 30 min, the sections were incubated with rabbit anti-TaeMCAII (Shanghai ImmunoGen Bio-technology, China) at a 1 : 100 dilution for 2.5 h at 37 ℃. The slides were incubated in a biotinylated goat-anti-rabbit antibody (ZSGB-BIO; 1 : 300) in PBS for 30 min at 37 ℃, then stained with DAB (DAB kit, ZSGB-BIO) according to the manufacturer's instructions. A brown signal was viewed under a light microscope (Nikon Eclipse 80i, Japan) and photographed. The specificity of the polyclonal antibody was analysed by a normal Western blot.

The control group used the phosphate buffer solution (PBS) instead of the rabbit anti-TaeMCAII.

Immunoelectron microscopy of TaeMCAII

Immune-electron microscopy was used according to Cai's method (Cai et al. 2015). The sections (80–90 nm thick) were cut on an LKB 2088 Ultracut ultramicrotome (Bromma, Sweden) and incubated with rabbit anti-TaeMCAII (Shanghai ImmunoGen Bio-technology, China), then stained with 2% lead citrate and uranyl acetate, and examined with a TEM (H-7650, Hitachi, Japan) at 80 kV.

The control group used the bull serum albumin solution instead of the rabbit anti-TaeMCAII.

Results

The microstructure and ultrastructure of the development of SEs in wheat caryopses

As the SEs developed, the microstructures revealed that the number of SEs increased gradually in the abdominal vascular tissue of wheat caryopsis (Fig. 1a and Fig. 1b). The ultrastructures exhibited the following dynamic changes of the development of wheat SEs at the subcellular level: enucleantion, inclusion loss, cell wall thickening and decreased (Fig. 2) cytosol density. These observations indicated that wheat caryopsis had two obvious levels of development: the tissue level that showed the cell number increases which aided the transportation of nutrition in the gain filling, and the subcellular level that showed PCD-like cell organelles degradation.

Nuclear DNA degradation

The TUNEL results determined no positive labeling (indicated by green fluorescence) at 2 DAF, 5 DAF, 6 DAF and 7 DAF (Fig. 3A, D, E, F). The green fluorescence was only observed at 3 DAF and 4 DAF, indicating that the nuclear degradation occurred during these periods (Fig. 3B, C). The PI staining showed that the number of nuclei indicated by the red fluorescent signal increased in the SE clusters at 2 DAF and 3 DAF (Fig. $3a_2$, b_2), decreased slightly at 4 DAF (Fig. $3c_2$), and then maintained the same amounts at 5 DAF, 6 DAF and 7 DAF (Fig. $3d_2$, e_2, f_2). The number of the red fluorescence nuclei was stable for the cells in addition to the SEs (Fig. $3a_2$, b_2, c_2, d_2, e_2, f_2).

TaeMCAII mRNA dynamic changes in the development of the SEs

The expression levels of the gene encoding TaeMCAII displayed dynamic changes during the development of wheat SEs at 0–7 DAF (Fig. 4). From 0–3 DAF, the expression levels of the gene encoding TaeMCAII increased gradually and reached the second highest level at 3 DAF, and then decreased at 4–6 DAF. At 7 DAF, the expression levels sharply increased, indicating that TaeMCAII was still functional late in the development of SEs.

The localization of TaeMCAII mRNA in the abdominal vascular tissue of caryopses by in situ hybridization displayed the strongest blue signal appearing in the SEs at 3 DAF and 4 DAF (Fig. 5C, D), and decreased at 5 DAF (Fig. 5E), but gradually increased at 6 DAF and 7 DAF (Fig. 5F, G). No label appeared in the control at 4 DAF (Fig. 5H). These results were consistent with previous q-PCR results.

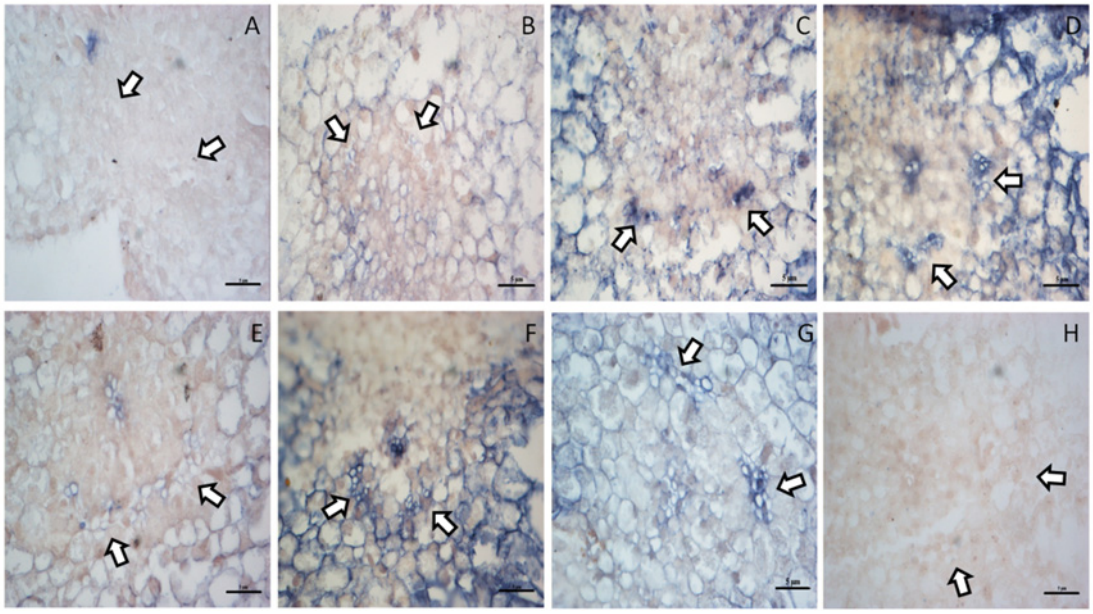

Fig. 5. Localization of TaeMCAII mRNA in abdominal vascular tissue of caryopses by *in situ* hybridization. A–G represent the cross section at 1 DAF to 7 DAF, respectively, which were treated with antisense probes. No signal appeared at 4 DAF (H), which was treated with sense probes. Arrows show the SEs clusters. Bar: 5 μm.

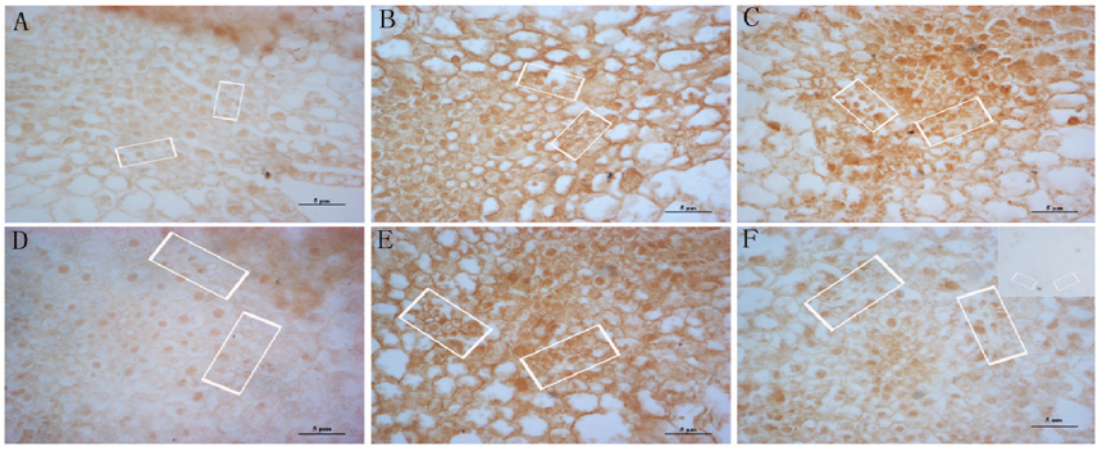

Fig. 6. Immunohistochemical localization of TaeMCAII in SEs. A–F represent the cross section at 2 to 7 DAF, respectively, the boxes show the SEs clusters. No label appeared in the negative at 4 DAF (Top right corner of F), Bar: 5 μm.

Immunohistochemistry and immunoelectron microscopy localization

TaeMCAII

The above q-PCR results revealed that with the development of SEs, the expression levels of the gene coding TaeMCAII experienced dynamic changes, indicating that TaeMCAII might play an important role in the development of SEs. But, the q-PCR results only showed the transcription level changes of TaeMCAII. Thus, immunohistochemical localization of TaeMCAII was used to further study the dynamic changes of TaeMACII at the protein level in the development of wheat SEs. Tests of the rabbit anti-TaeMCAII showed the antibody could be used in this study (Appendix 1). The immunohistochemical localization of TaeMCAII displayed the strongest brown signal in the SEs at 3 DAF and 4 DAF (Fig. 6B, C), and decreased at 5 DAF (Fig. 6D), but the brown signal gradually increased at 6 DAF and 7 DAF (Fig. 6E, F), which indicated that the protein was also expressed in late development of SEs.

The immunohistochemical localization of TaeMCAII showed the dynamic changes of TaeMCAII only at the tissue level. Next, subcellular localization of TaeMCAII by immunoelectron microscopy was detected to better understand the possible mechanisms and processes involved in the development of wheat SEs and their significance in SEs-semi-death. TaeMCAII was localized as black colloidal gold particles. At 1 DAF, few colloidal gold particles were observed in the nucleus (Fig. 7A, a_1, a_2). At 2 DAF, the colloidal gold particles began to increase, and continued to be observed in the nucleus, which indicated a condensed state (Fig. 7B, b_1). The intensity of the gold particles was strongest at 3 DAF, and an abundance of gold particles were distributed in the cytoplasm and in the frag-

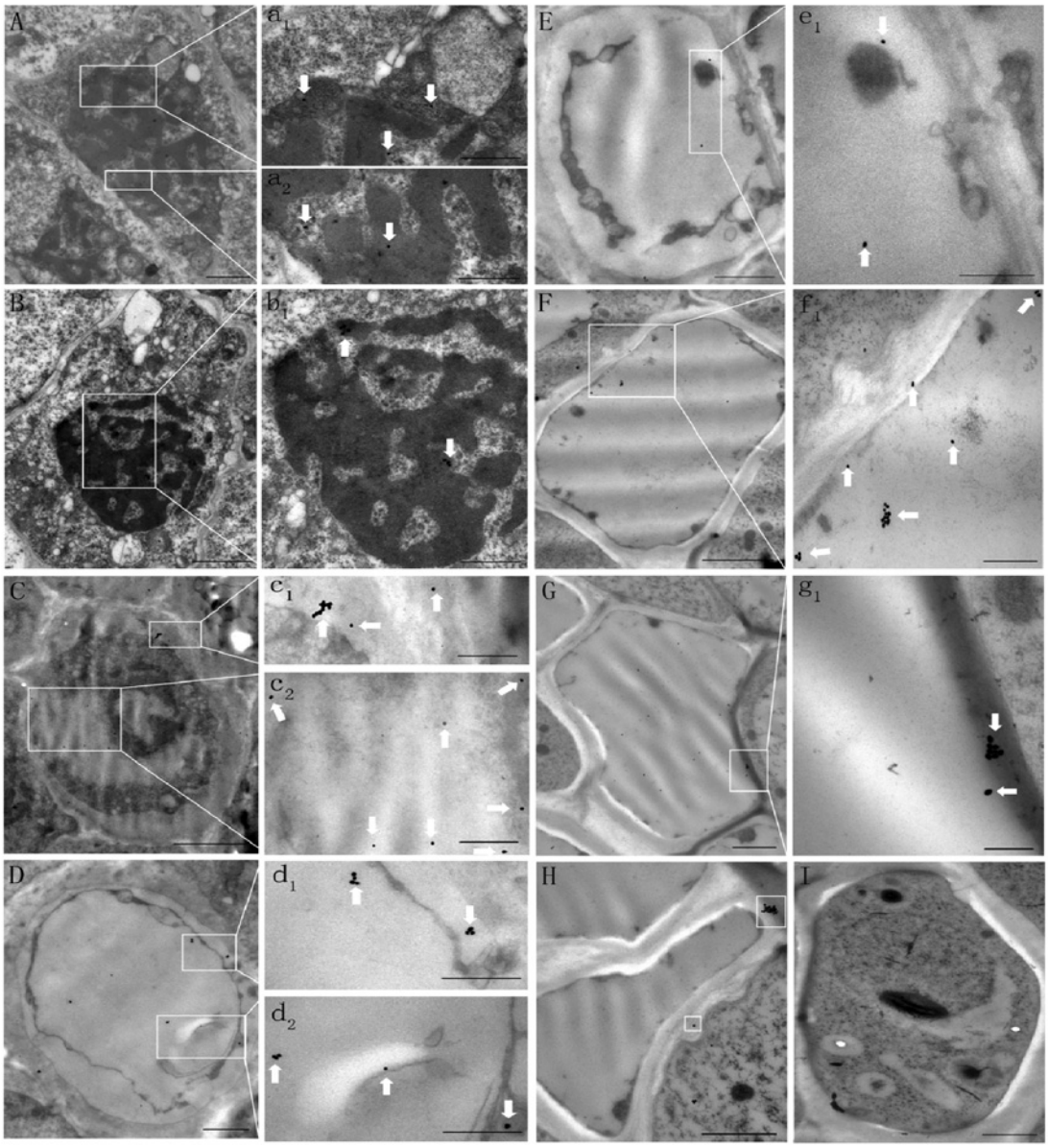

Fig. 7. Subcellular localization of TaeMCAII by immunoelectron microscopy in SEs of wheat caryopsis. The white arrows show the gold particles which represent the TaeMCAII. a_1, a_2, b_1, c_1, c_2, d_1, d_2, e_1, f_1 and g_1 are the enlarged areas of the white boxes in A-G, respectively. A, a_1, a_2: 1 DAF. B, b_1: 2 DAF. C, c_1, c_2: 3 DAF. D, d_1, d_2: 4 DAF. E, e_1: 5 DAF. F, f_1: 6 DAF. G, H, g_1: 7 DAF. No gold particles appeared in the negative control at 4 DAF (I). Bar: 200 nm (g_1), Bar: 1 μm (A, B, D, E, G, H, I), Bar: 0.5 μm (a_1, a_2, b_1, c_1, c_2, d_1, d_2, e_1, f_1), Bar: 2 μm (C, F).

mented nucleus. The cytoplasm also appeared the electron transparent area near the fragmented outer nuclear membrane, which indicated signs of cell disintegration (Fig. 7C, c_1, c_2). At 4 DAF, the gold particles were distributed in the fragments of the nuclei (Fig. 7D, d_1, d_2), had decreased the cytosol density, and approached the vacuolar membrane to the plasma membrane. With the rupture of the vacuolar membrane, a number of gold particles were detected only in the cytoplasm at 5 DAF (Fig. 7E, e_1). At 6 DAF, the gold particles were mainly distributed around the inner cell wall (Fig. 7F, f_1). At 7 DAF, most gold particles were concentrated in the cell wall, and a few were also observed in the cytoplasm (Fig. 7G, H, g_1). No gold particles were observed in the negative control at 4 DAF (Fig. 7I).

Discussion

Plants reshape their organizational structure to complete normal development and to adapt to environmental changes by PCD, such as leaf senescence (Gan & Amasino 1997), the formation of catheter (Zhang et al. 2002) and aleurone (Wang et al. 1996b) and the development of calyptras (Møller & McPherson 1998). The development of SEs occurred primarily between 0 DAF-7 DAF in wheat caryopsis, and the microstructure indicated that the development of wheat SEs was a two-level process: the tissue level, which had cell number increases, and the subcellular level, in which PCD-like cell organelles degradation, such as enucleation, partial inclusions deletion, thick cell walls, and cytoplasm elec-

tronic transparency were observed. The TUNEL results showed that nuclear DNA fragmentation also occurred. These results indicated that the development of SEs shared some features of the PCD process, but the SEs were being alive at the end. Therefore, the development of SEs is a special formed PCD that builds the organic nutrient transport channel.

Metacaspases were reported to function in plants as a defense (Coll et al. 2010; Watanabe & Lam 2011a) to UV-induced cell death (He et al. 2008) and to the PCD process of European spruce embryo formation (Suarez et al. 2004). However, their specific functions and the substrates are not fully understood. The q-PCR and situ hybridization showed that TaeMCAII exhibited a dynamic trend in the development of SEs, and were primarily expressed at 3 DAF and 4 DAF, which coincided with the nuclear DNA fragmentation. The results of the immunoelectron microscope showed that the dynamic changes of TaeMCA II appeared in three stages. In the first stage, at 1 DAF and 2 DAF, TaeMCAII was mainly localized in the nucleus. In the middle stage starting at 3 DAF, 4 DAF and 5 DAF, the protein concentration increased, and was generally distributed in the cytoplasm and around the fracture of nuclear debris. The last stage, which started at final phase of the development of the SEs, showed observable translocation of TaeMCAII from the cytoplasm to the cell wall, and the protein content increased. The dynamic changes of TaeMCAII showed similar localization patterns to Ca^{2+} during the development of SEs in our previous reported studies. During early differentiation periods of the SEs (1 DAF and 2 DAF), Ca^{2+} was primarily distributed in the cell membrane and the nucleus. With the progress of the PCD (4 DAF), the Ca^{2+} concentration increased in cytoplasm. When the PCD ceased (5 DAF and 6 DAF), Ca^{2+} transferred from the cytoplasm to the cell wall (Li 2009). This indicated that TaeMCAII co-localized with Ca^{2+} in the development of SEs. As one of the core components in the eukaryotic cell signal transduction, Ca^{2+} has important implications in regulating the growth, development, metabolism and physiological functions in plants. The increased Ca^{2+} concentrations in cytoplasm activated endonuclease that resulted in DNA fragmentation, and led to the occurrence of PCD, but the phenomenon disappeared after the addition of endonuclease inhibitors (Jones et al. 1989). It should be noted that the high levels of Ca^{2+} required for the optimal activity of the wheat metacaspase TaeMCAII and other plant metacaspases, such as AtMC4 and mcIIPa, might play significant roles in the adaptation and acclimation of these plants to stressful environmental conditions (Piszczek et al. 2012). Thus, it is inferred that the activity of TaeMCAII might be dependent on Ca^{2+} and have an additional function in nucleus degradation.

Interestingly, TaeMCAII did not lose its activity at the end of the SEs' PCD process. On the contrary, its expression levels increased, and a subcellular localization showed that TaeMCAII was primarily distributed near the cell wall at the end of SE development. Previous results showed that SEs lost their nuclei and most of the organelles at the end of its development. Thus, we cannot help asking the following questions: Where does the TaeMCAII come from in the late stage of SE development? Does it have other effects other than to promote death? As previously mentioned, the developed SEs were not a typical PCD, the mature SEs still retained some organelles, and the cells were still active at the end of the development period. Therefore, the SEs required a variety of proteins and other biological macromolecules to maintain their activity. Early studies found that SEs and companion cells were closely linked through plasmodesmata during phloem development. The density of ribosomal was very low in the mature SEs, and the companion cells synthesized protein for the SEs (Richard 1997). Therefore, we hypothesized that the TaeMCAII may have originated from the companion cells during late SEs development.

Reverse genetic analysis shows that cell death regulation is just one of the multifaceted abilities of metacaspases, which can also control other biological processes either related or unrelated to cell death (Tsiatsiani et al. 2011). A single metacaspase Yca1 found in budding yeast provides a striking example of a multifunctional protein, because apart from cell death activated under various settings, it Yca1 was also required for cell cycle regulation and for the clearance of protein aggregates (Bozhkov et al. 2010). A recent study also documented the antagonistic functions of two Arabidopsis type I metacaspases, AtMC1 and AtMC2, in mediating hypersensitive response (HR)-associated cell death (Coll et al. 2010). This data indicated that the metacaspases might have different functions in organisms. Moreover, different genes or proteins are not completely isolated, as they affect each other though the mutual regulation and interaction to complete biological processes. Therefore, we hypothesized that TaeMCAII participated in the PCD and in certain functions in late nutrient transport in SEs.

Acknowledgements

Our deepest gratitude goes first and foremost to the National Nature Science Foundation of China (31171469; 31471428). Moreover, our sincere thanks to Q.T. Xu, M. Y, C.Y. Li, Y.H. Qi.

References

Bozhkov P.V., Smertenko A.P. & Zhivotovsky B. 2010. Aspasing out metacaspases and caspases: proteases of many trades. Sci. Signal. **3:** 48.

Bozhkov P.V., Suarez M.F., Filonova L.H., Daniel G., Zamyatnin A.A., Rodriguez-Nieto J.S., Zhivotovsky B. & Smertenko A. 2005. Cysteine protease mcII-Pa executes programmed cell death during plant embryogenesis. Proc. Natl. Acad. Sci. USA **102:** 14463–14468.

Cai J.T., Zhang Z.H., Zhou Z.Q., Yang W.L, Liu Y., Mei F.Z., Zhou G.S. & Wang L.K. 2015. Localization of BEN1-LIKE protein and nuclear degradation during development of metaphloem sieve elements in *Triticum aestivum* L. Acta Biol. Hung. **66:** 66–79.

Castillo-Olamendi L., Bravo-García A., Morán J., Rocha-Sosa M. & Porta H. 2007. AtMCP1b, a chloroplast-localised metacaspase, is induced in vascular tissue after wounding or pathogen infection. Funct. Plant Biol. **34:** 1061–1071.

Choi C.J. & Berges J.A. 2013. New types of metacaspases in phytoplankton reveal diverse origins of cell death proteases. Cell Death Differ. **4:** e490.

Coll N.S., Vercammen D., Smidler A., Clover C., Van Breusegem F., Dangl J.L. & Epple P. 2010. Arabidopsistype I metacaspases control cell death. Science **330:** 1393–1397.

Earnshaw W.C., Martins L.M. & Kaufmann S.H. 1999. Mammalian caspases: structure, activation, substrates and functions during apoptosis. Annu. Rev. Biochem. **68:** 383–424.

Gan S. & Amasino R.M. 1997. Making sense of senescence. Molecular genetic regulation and manipulation of leaf senescence. Plant Physiol. **113:** 313–319.

Guo Y.J. 2013. Influence of Caspase 3-like proteases on programmed cell death of endosperm cells in winter wheat (*Triticum aestivum* L.) under waterlogging. Dissertation, Huazhong Agricult Univ, China.

Hao X., Qian J., Xu S., Song X. & Zhu J. 2008. Location f caspase 3-like protease in the development of sieve element and tracheary element of stem in *Cucurbita moschata*. J. Integ. Plant Biol. **50:** 1499–1507.

He R., Drury G.E., Rotari V.I., Gordon A., Willer M., Farzaneh T., Woltering E.J. & Gallois P. 2008. Metacaspase-8 modulates programmed cell death induced by ultraviolet light and H_2O_2 in Arabidopsis. J. Biol. Chem. **283:** 774–783.

Jones A.M. 2001. Programmed cell death in development and defense. Plant Physiol. **125:** 94–97.

Jones A.M. & Dangl J.L. 1996. Logiam at the Styx: Programmed cell death in plants. Trends Plant Sci. **l:** 114–119.

Jones D.P., McConkey D.J., Nieotera P. & Orrenius S. 1989. Caleium-activated DNA fragmentation in rat liver nuclei. J. Biol. Chem. **264:** 6398–640.

Li J.W. 2009. Locaization of Ca^{2+} and related enzymes in phloem in the developing caryopsis of *Triticum aestivum* L. Dissertation, Huazhong Agricult. Univ., China.

McLuskey K., Rudolf J., Proto W.R., Isaacs N.W., Coombs G.H., Moss C.X. & Mottram J. C. 2012. Crystal structure of a *Trypanosoma brucei* metacaspase. Proc. Natl. Acad. Sci. USA **109:** 7469–7474.

Møller S.G. & McPherson M.J. 1998. Developmental expression and biochemical analysis of the Arabidopsis atao1 gene encoding an H_2O_2-generating diamine oxidase. Plant J. **13:** 781–791.

Pennell R.I. & Lamb C. 1997. Programmed cell death in plants. Plant Cell **9:** 1157–1168.

Piszczek E., Dudkiewicz M. & Mielecki M. 2012. Biochemical and bioinformatic characterization of type II metacaspase protein (TaeMCAII) from wheat. Plant Mol. Biol. Rep. **30:** 1338–1347.

Piszczek E., Dudkiewicz M. & Sobczak M. 2011. Molecular cloning and phylogenetic analysis of cereal type II metacaspase cDNA from wheat. Biol. Plantarum **55:** 614–624.

Piszczek E. & Gutman W. 2007. Caspase-like proteases and their role in programmed cell death in plants. Acta Physiol. Plant. **29:** 391–398.

Richard D.S. 1997. The phloem sieve element: a river runs through it. Plant Cell **9:** 1137–1146.

Sanmartin M., Jaroszewski L., Raikhel N.V. & Rojo E. 2005. Caspases. Regulating death since the origin of life. Plant Physiol. **137:** 841–847.

Suarez M.F., Filonova L.H., Smertenko A., Savenkov E.I., Clapham D.H., Von Arnold S., Zhivotovsky B. & Bozhkov P.V. 2004. Metacaspase dependent programmed cell death is essential for plant embryogenesis. Curr. Biol. **14:** 339–340.

Sun Y. 1998. Progress in calcium signaling of the cell nuclei. Plant Biol. **20:** 133–137.

Tsiatsiani L., Van Breusegem F., Gallois P., Zavialov A., Lam E. & Bozhkov P.V. 2011. Metacaspases. Cell Death Differ. **18:** 1279–1288.

Uren A.G.O., Rourke K. & Aravind L.A. et al. 2000. Identification of Paracaspases and Metacaspase: two ancient families of Caspase-like proteins, one of which plays a key role in MALT lymphoma. Mol. Cell. **6:** 961–967.

Van Bel A.J.E. 2003. The phloem, a miracle of ingenuity. Plant Cell Environ. **26:** 125–149.

Wang L.K., Zhou Z.Q., Song X.F., Li J.W., Deng X.X. & Mei F. Z. 2008. Evidence of ceased programmed cell death in metaphloem sieve elements in the developing caryopsis of *Triticum aestivum* L. Protoplasma **234:** 87–96.

Wang M., Oppedijk B.J., Lu X., Van Duijn B. & Schilperoort R.A. 1996b. Apoptosis in barley aleurone during germination and its inhibition by abscisic acid. Plant Mol. Biol. **32:** 1125–1134.

Watanabe N. & Lam E. 2011a. Arabidopsis metacaspase 2d is a positive mediator of cell death induced during biotic and abiotic stresses. Plant J. **66:** 969–982.

Watanabe N. & Lam E. 2011b. Calcium-dependent activation and autolysis of Arabidopsis metacaspase 2d. J Bio. Chem. **286:** 10027–10040.

Wong A.H.H., Yan C. & Shi Y. 2012. Crystal structure of the yeast metacaspase Yca1. J. Biol. Chem. **287:** 29251–29259.

Xu Q.T., Yang L., Zhou Z.Q., Mei F.Z., Qu L.H. & Zhou G.S. 2013. Process of aerenchyma formation and reactive oxygen species induced by waterlogging in wheat seminal roots. Planta **238:** 969–982.

Yang W.L. 2013. Study on Programmed Cell Semi-Death of Sieve Elements in Root and Developing Caryopsis of *Triticum aestivum* L. Dissertation, Huazhong Agricult. Univ., China.

Zhang X., Coté G. & Crain R. 2002. Involvement of phosphoinositide turnover in tracheary element differentiation in *Zinnia elegans* L. cells. Planta **215:** 312–318.

Zhang Y. & Lam E. 2011. Sheathing the swords of death. Post-translational modulation of plant metacaspases. Plant Signal Behav. **6:** 2051–2056.

Zhou Z.Q., Lan S.Y., Zhu X.T., Wang W.J. & Xu Z.X. 2004. Utrastructure and its function of phloem cell in abdominal vascular bundle of wheat caryopsis. Acta Agron. Sin. **30:** 163–168.

Received August 30, 2016
Accepted December 28, 2016